Appl. Phys. A 79, 507–514 (2004)
DOI: 10.1007/s00339-003-2480-2

Applied Physics A
Materials Science & Processing

S. PLEASANTS[1,✉]
N. ARNOLD[2]
D.M. KANE[1]

Acoustic substrate expansion in modelling dry laser cleaning of low absorbing substrates

[1] Department of Physics, Macquarie University, NSW 2109, Sydney, Australia
[2] Angewandte Physik, Johannes-Kepler-Universität, 4040 Linz, Austria

Received: 5 August 2003/Accepted: 13 November 2003
Published online: 11 February 2004 •

ABSTRACT Acoustic expressions have been derived for the thermal expansion of substrate surfaces due to irradiation by an exponential laser pulse. The result of acoustic effects on three substrates (silicon, glass and silica) with different absorptions has been calculated.

It has been shown that for substrates having relatively low absorptions, like silica and glass, acoustic considerations substantially reduce thermal expansion of the substrate caused by irradiation by nanosecond laser pulses relative to a quasi-static expansion model. In particular, the expansion of the substrate occurs over a much longer time frame than when the quasi-static approximation holds. Consequently, acceleration of the substrate surface is greatly reduced and laser cleaning threshold fluences for particle removal are increased.

The predictions of the model of Arnold et al. when developed for acoustic considerations give reasonable agreement with experimentally found threshold fluences for alumina particles on silica and glass substrates although it underestimates the ratio of the threshold cleaning fluences of silica and glass. This could be due to the model underestimating the contribution of surface expansion to the laser cleaning process. The influence of multiple reflections in the substrate and departure from one dimensionality in the heat conduction on the threshold fluence was found to be insignificant. Thermal contact between the particle and the substrate was also found to have little effect on laser cleaning threshold fluences. Another mechanism that may enhance surface expansion is the 3D focussing of radiation by the particles.

PACS 42.62.Cf; 81.65.Cf; 42.55.Lt

1 Introduction

Laser cleaning is one of a range of techniques for removing contamination from surfaces. Dry laser cleaning offers advantages over other cleaning techniques through being fast and a non-contact cleaning process that does not require the use of solvents. It can also be spatially selective if required. Laser cleaning has been demonstrated to clean both metallic and non-metallic surfaces and to remove particles as small as 65–80 nm in diameter [1]. On glass surfaces, removal of particles as small as 0.3 μm has been demonstrated [2–4].

✉ Fax: +61-2/9850-8115, E-mail: spleasan@physics.mq.edu.au

There have been several reports of models of the dry laser cleaning process [5–11]. The vast majority of them are based on thermal expansion of either the substrate or the particles. Most of the models are 1D and tend to overestimate threshold fluences by 1–2 orders of magnitude [12].

Luk'yanchuk, Zheng and Lu have developed a model that accounts for the field enhancement effect, 3D thermal elasticity and true pulse shape which predicts threshold fluences of the correct order of magnitude as those observed in experiments [12]. A similar model presented by Arnold et al. [13–15] also represents a substantial advancement over earlier models that appeared in the literature. It treats the particle and substrate expansion in a unified manner. This was shown to be important in the modelling of laser cleaning of alumina from silica and glass substrates since neither particle expansion nor substrate expansion by themselves could adequately explain the experimental results [16]. Both models account for the elasticity of the particle and substrate.

Arnold et al. showed that the expansion of the substrate will depend on the relative size of the laser spot, the distance travelled by sound, and the temperature distribution generated by the absorption of the short laser pulse. In particular, the problem can be considered as being one dimensional if both the heat and the sound are contained within the lateral dimension of the laser spot, w_0, i.e. if $l_\mathrm{T} \ll w_0$ and $\nu_\mathrm{s}\tau \ll w_0$, where l_T is the thermal diffusion length [17] and ν_s is the speed of sound in the substrate and τ is the laser pulse length (see Fig. 1).

The determination of whether a particular substrate system should be treated dynamically or quasi-statically requires comparison of the relative dimensions of the heated volume and the distance travelled by sound in the axial direction. If the sound leaves the heated region in the axial direction, i.e. if $\nu_\mathrm{s}\tau \gg l_\alpha + l_\mathrm{T}$ where l_α is the absorption length for the radiation, then the quasi-static approximation holds. This is the case that was derived in [13–15]. The displacement of the substrate surface from its initial position $l(t)$ is then proportional to the fluence absorbed up to the current moment, $\phi_\mathrm{a}(t) \equiv \int_0^\mathrm{t} I_\mathrm{a}(t_1)\mathrm{d}t_1$, where I_a is the absorbed laser intensity. For the purely 1D case with $\nu_\mathrm{s}\tau \ll w_0$, the displacement is given by:

$$l(t) = \frac{1+\sigma_\mathrm{s}}{1-\sigma_\mathrm{s}} \frac{\beta_\mathrm{s}}{3c_\mathrm{s}\varrho_\mathrm{s}} \phi_\mathrm{a}(t)\,, \tag{1}$$

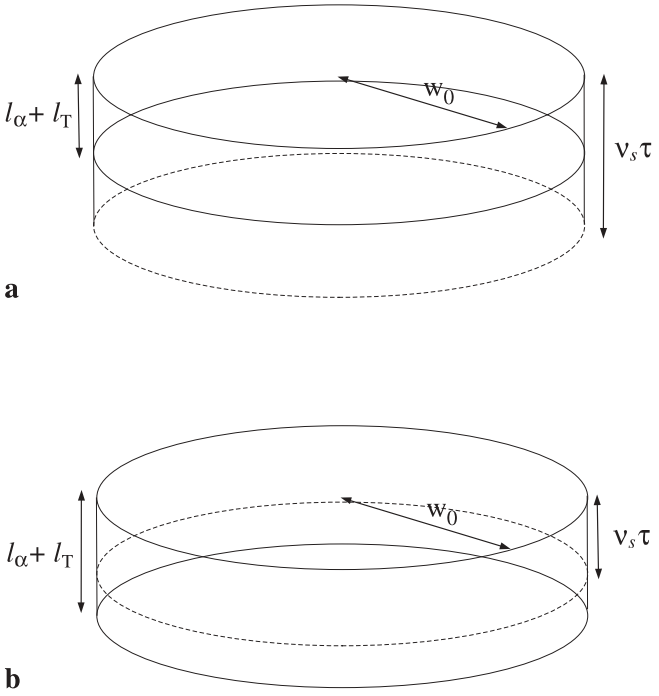

FIGURE 1 Schematic diagram showing the relative dimensions of the heat and sound in the substrate; **a** is the quasi-static unilateral expansion case while **b** is the dynamic unilateral expansion case [13]

where σ is the Poisson ratio, β is the coefficient of volumetric expansion, c is the specific heat capacity and ϱ is the density. The subscript s denotes the substrate.

If, however, the sound does not leave the heated region in the axial direction ($\nu_s\tau < l_\alpha$) then the elastic problem needs to be treated dynamically. This case is considered in the next section.

In general for substrates with high absorption like silicon (coefficient of absorption at wavelength $\lambda = 248\,\text{nm}$, $\alpha_s = 1.67 \times 10^8\,\text{m}^{-1}$), the quasi-static approximation is valid. However this will not be the case for substrates like microscope slide glass ($\alpha_s = 5185\,\text{m}^{-1}$) and fused silica ($\alpha_s = 3.2\,\text{m}^{-1}$). In these cases the problem should be treated dynamically as will be demonstrated below.

2 Derivation of a dynamic expression for substrate expansion

The displacement of the substrate is governed by the one-dimensional equation of thermoelasticity,

$$\frac{\partial^2 u}{\partial t^2} = \nu_s^2 \frac{\partial^2 u}{\partial z^2} - \frac{\beta_s}{3\varrho_s} \frac{E_s}{(1-2\sigma_s)} \frac{\partial T_s}{\partial z}\,, \tag{2}$$

where $u(z,t)$ is the z component of the displacement of the substrate, E_s is Young's modulus and $T(z,t)$ is the axial temperature distribution in the substrate, relative to the ambient temperature. The boundary condition for a free surface at $z = 0$ is:

$$\sigma_{zz} = \nu_s^2 \frac{\partial u}{\partial z} - \frac{\beta_s}{3\varrho_s} \frac{E_s}{(1-2\sigma_s)} T_s = 0\,, \tag{3}$$

where σ_{zz} is the longitudinal stress and ν_s is the longitudinal sound velocity in the substrate, given by

$$\nu_s = \sqrt{\frac{E_s(1-\sigma_s)}{\varrho_s(1+\sigma_s)(1-2\sigma_s)}}\,. \tag{4}$$

Combining this with (2) the following result for the displacement of a free surface can be obtained [13, 14, 18]:

$$l(t) = -u(z=0,t) = \beta_l \int_0^{\nu_s t} T_s(z, t - z/\nu_s)\,\mathrm{d}z \quad \text{for} \quad t \le d/\nu_s \tag{5}$$

where d is the thickness of the substrate and β_l is the coefficient of unilateral thermal expansion

$$\beta_l = \frac{\beta_s}{3}\frac{1+\sigma_s}{1-\sigma_s}\,. \tag{6}$$

The limit of (5) as $\nu_s \to \infty$ gives the static result for the surface displacement [14], namely

$$l(t) = \beta_l \int_0^{\infty} T_s(z,t)\,\mathrm{d}z\,. \tag{7}$$

The physical meaning of (5) is that the information about the thermal expansion of the sub-surface layers cannot reach the surface with a velocity faster than that of sound. Thus, only the region $0 < z < \nu_s t$ influences the expansion at the time t.

The temperature distribution in the substrate is determined by the one-dimensional heat equation [17]

$$c_s\varrho_s \frac{\partial T_s}{\partial t} - \frac{\partial}{\partial z}\left[k_s \frac{\partial T_s}{\partial z}\right] = (1-R_s)\ \alpha_s e^{-\alpha_s z} I(t)\,, \tag{8}$$

where R_s is the Fresnel reflectivity from a single interface and k_s is the thermal conductivity of the substrate and $I(t)$ is the time dependent intensity of the laser radiation. For short time scales, heat conduction is negligible and it is possible to neglect the second term on the left hand side. For nanosecond pulse lengths usually employed in laser cleaning for weak absorbers, this is an excellent approximation as long as $l_T \ll l_\alpha$.

Indeed, over the time scale t, the first term is of the order of $c_s\varrho_s T/t$ while the second term is of the order of $k_s T/l^2$, where l is the typical length scale, given by the absorption length in our case. Thus, their ratio is about $1/\alpha_s^2 D_s t$, where D_s is the thermal diffusivity. This is about $6.4 \times 10^6 \gg 1$ for glass slides and $t \approx 10\,\text{ns}$ (approximate time scale of laser pulse) and is even larger for weaker absorbing silica. Thus, the heat conduction term can be neglected and the temperature can be calculated using the calorimetric approximation. Similarly, after the end of laser pulse the axial equalization of temperature within the specimen will take place on the time scale $t \approx \alpha_s^2 D_s \approx 25\,\text{s}$. This time is much longer than the time needed for sound to travel through the thickness of the glass slide, and longer than all other relevant time scales of the problem. In reality, at such times, 3D effects and heat exchange with the surrounding (neglected in the present treatment) will start to play a role.

Ignoring the conduction term in (8) and integrating with respect to time gives

$$T_s(z,t) = (1-R_s)\frac{\alpha_s e^{-\alpha_s z}}{c_s \varrho_s}\phi(t) \quad \text{for } 0 \le z \le d\,. \tag{9}$$

Substituting this expression into (5) gives

$$l(t) = (1-R_s)\frac{\beta_l}{c_s\varrho_s}\int_0^{\nu_s t}\alpha_s e^{-\alpha_s z}\phi(t-z/\nu_s)\,\mathrm{d}z \quad \text{for } t \le d/\nu_s\,. \tag{10}$$

Changing the variable of the integral and integrating by parts results in the following expression for the displacement of the substrate

$$l(t) = (1-R_s)\frac{\beta_l}{c_s\varrho_s}\left(\phi(t) - \int_0^t e^{\alpha_s\nu_s(t_1-t)}I(t_1)\,\mathrm{d}t_1\right) \quad \text{for } t \le d/\nu_s\,. \tag{11}$$

For a pulse shape described by

$$I_{\exp}(t) = I_0\frac{t}{\tau}\exp\left(-\frac{t}{\tau}\right)\,, \tag{12}$$

(11) becomes

$$l(t) = (1-R_s)\frac{\beta_l}{c_s\varrho_s} \times \left\{\phi_{\exp}(t) - \frac{e^{-\alpha_s\nu_s t}}{\gamma_d^2}I_0\tau e^{-\gamma_d t/\tau}(e^{\gamma_d t/\tau} - \gamma_d t/\tau - 1)\right\} \quad \text{for } t \le d/\nu_s\,, \tag{13}$$

where $\phi_{\exp}(t)$ is the time dependent fluence of the pulse shape given in (12) and $\gamma_d = 1-\alpha_s\nu_s\tau$. It can be expressed more simply as

$$l(t) = (1-R_s)\frac{\beta_l}{c_s\varrho_s}\left\{\phi_{\exp}(t) - \frac{e^{-\alpha_s\nu_s t}}{\gamma_d^2}\phi_{\exp}(\gamma_d t)\right\} \quad \text{for } t \le d/\nu_s\,. \tag{14}$$

Here the term $\phi_{\exp}(\gamma_d t)$ does not have a direct physical interpretation, it merely serves as a convenient shorthand.

3 A comparison of the thermal expansion of three different substrates

The magnitude of the dimensionless quantity γ_d determines the degree of departure from the quasi-static approximation. For highly absorbing substrates, γ_d will be a large negative number. In this case, the last term in (14) can be neglected and the substrate expansion will be described well by the quasi-static approximation (compare with (1)). For low absorbing substrates, γ_d will be close to 1 and then the sound-related effects will dominate the dynamics of substrate expansion.

The effect of γ_d on the substrate expansion can be illustrated by considering three different substrates, namely silicon, glass and silica. Table 1 shows the absorption coefficient at 248 nm and γ_d (for $\tau = 8.1$ ns, i.e., $\tau_{FWHM} = 20$ ns) for these three substrates. Silicon is highly absorbing at this wavelength, silica is almost transparent, while glass is considerably more absorbing than silica.

Substrate	α (m^{-1})	γ_d
Silicon	1.67×10^8	-12610
Glass	5185	0.7666
Silica	3.2	0.9998

TABLE 1 Values of the absorption coefficient at 248 nm and γ_d (with τ = 8.1 ns) for silicon, glass and silica

It should be noted that while for silicon the thermal diffusion distance exceeds the radiation absorption depth, thermal conductivity doesn't affect the expansion of the surface. This is because the distance that heat travels during the laser pulse is smaller than the distance sound travels for the duration of the laser pulse and the quasi-static approximation holds. Since the sound from the heated subsurface region can reach the surface during the laser pulse the surface expansion is not affected by thermal conductivity [13–15].

For the purpose of comparison, substrate displacement divided by the maximum quasi-static substrate displacement for all three substrates has been plotted in Fig. 2. The displacement of silicon is the same as that calculated using the quasi-static approximation and is proportional to the transient fluence. The displacement of microscope slide glass rises more slowly than that of silicon, while pure silica's displacement is almost negligible in comparison.

Since silicon is well described by the quasi-static approximation, the very substantial difference between its thermal expansion and that of microscope slide glass and fused silica demonstrates that for substrates with low absorption it is important to take the finite velocity of sound into account when modelling substrate expansion.

4 Effect of dynamic considerations on the threshold fluences for laser cleaning of alumina from silica and glass

This section examines the effect that a dynamic treatment of substrate expansion has on the threshold fluence for laser cleaning of alumina particles from microscope slide glass and silica substrates. Tables 2, 3 and 4 give the values of the relevant material properties for alumina, glass and silica. Microscope slide glass and silica have essentially identical physical and optical properties except that microscope slide glass is considerably more absorbing than silica and has a higher coefficient of thermal expansion.

Specific heat, c_p	754 J kg^{-1} K^{-1}
Volumetric thermal expansion, β_p	26.4×10^{-6} K^{-1}
Poisson ratio, σ_p	0.22
Young modulus, E_p	435×10^9 Nm^{-2}
Density, ϱ_p	4000 kg m^{-3}
Absorptivity, A_p	0.16
Particle size, r	3.0 μm
Contact radius, a	36 nm
Work of adhesion (with glass/silica), φ	0.0995 J m^{-2}

TABLE 2 Material values for the alumina particles (contact radius was estimated, other values were taken from [19])

Specific heat, c_s	$772\,\mathrm{J\,kg^{-1}\,K^{-1}}$
Volumetric thermal expansion, β_s	$212.1\times10^{-7}\,\mathrm{K^{-1}}$
Poisson ratio, σ_s	0.17
Young's modulus, E_s	$7.0\times10^{10}\,\mathrm{Nm^{-2}}$
Density, ϱ_s	$2437\,\mathrm{kg\,m^{-3}}$
Speed of sound, ν_s	$5556\,\mathrm{m\,s^{-1}}$
Absorption coefficient, α_s	$5185\,\mathrm{m^{-1}}$
Thermal conductivity, k_s	0.92 W/mK
Reflectivity, R_s	0.041
Diffusivity, D_s	$4.89\times10^{-7}\,\mathrm{m^2\,s^{-1}}$
Slide thickness, d	1.0 mm

TABLE 3 Material values for the glass microscope slides (The density was measured directly, thermal expansion and conductivity were averaged values taken from [25], the speed of sound, reflectivity and diffusivity were all calculated from other material parameters. Other values were taken from [19])

Specific heat, c_s	$772\,\mathrm{J\,kg^{-1}\,K^{-1}}$
Volumetric thermal expansion, β_s	$15.3\times10^{-7}\,\mathrm{K^{-1}}$
Poisson ratio, σ_s	0.17
Young's modulus, E_s	$7.0\times10^{10}\,\mathrm{Nm^{-2}}$
Density, ϱ_s	$2185\,\mathrm{kg\,m^{-3}}$
Speed of sound, ν_s	$5868\,\mathrm{m\,s^{-1}}$
Absorption coefficient, α_s	$3.2\,\mathrm{m^{-1}}$
Thermal conductivity, k_s	1.38 W/mK
Reflectivity, R_s	0.041
Diffusivity, D_s	$8.18\times10^{-7}\,\mathrm{m^2\,s^{-1}}$
Slide thickness, d	2.0 mm

TABLE 4 Material values for silica slides (The density and absorption were measured directly, the speed of sound, reflectivity and diffusivity were all calculated from other material parameters. Other values were taken from [19])

It is worth pointing out that the absorptivity of the alumina particles is difficult to measure due to the small size of the particles. Rough experimental estimates give a value of $A_p = 0.16$ [19]. This is many orders of magnitude larger than that expected for crystalline alumina which is rather transparent at 248 nm ($\alpha \approx 15\,\mathrm{m^{-1}}$ [20]). Such a value would result in an effective absorptivity of $A_p = \sigma_a/\pi r^2 = 4\times10^{-5}$ (calculated from cross section of spherical, weakly absorbing particle ((7.2) from [21]). The reason for this discrepancy is that the alumina used in this study is not crystalline. Rather, it is rough and is non-spherical in shape and is probably not stoichiometric. Thus, it is more strongly absorbing at this wavelength. Due to the poorly defined shape and uncertainties in the optical constants, we used experimental results from [19] as a guideline value for A_p.

The threshold fluence can be calculated by inserting (14) into the approximate equation of motion for the particle–substrate system as given in [13]:

$$\frac{\mathrm{d}^2h}{\mathrm{d}t^2}+\gamma\frac{\mathrm{d}h}{\mathrm{d}t}=\frac{1}{m_p}\left(2\pi r\phi-h^{\frac{3}{2}}r^{\frac{1}{2}}\bar{E}\right)+\frac{\mathrm{d}^2l}{\mathrm{d}t^2}+\frac{\mathrm{d}^2r}{\mathrm{d}t^2} \tag{15}$$

where r is the radius of the particle, ϕ is the work of adhesion between the particle and the substrate, γ is the damping coefficient, m_p is the mass of the particle, h is the total deformation of both the particle and the substrate and is given by

$$h(t)=l(t)+r(t)-x(t) \tag{16}$$

where x is the position of the center of the particle from the initial (non-deformed) substrate surface. Finally, $\bar{E}$ characterizes the elastic properties of the particle/substrate system and is defined as

$$\frac{1}{\bar{E}}=\frac{3}{4}\left(\frac{1-\sigma_p^2}{E_p}+\frac{1-\sigma_s^2}{E_s}\right). \tag{17}$$

Here σ is the Poisson ratio, E is the Young's modulus and the subscripts s and p denote the substrate and particle respectively.

The relationship between the radius of the particle and its temperature, which is assumed to be homogeneous, is given by

$$\dot{r}=\frac{\beta_p\dot{T}_p r}{3}. \tag{18}$$

The evolution of the particle temperature can be approximated by the following differential equation [13],

$$c_p m_p\frac{\mathrm{d}T_p}{\mathrm{d}t}=\sigma_a I-4K_s a(T_p-T_s), \tag{19}$$

where $\sigma_a \le \pi r^2 A_p$ is the absorption cross section and A_p is the absorptivity of the particle, a is the contact radius and T_s is the temperature of the substrate "far from the particle". For the case of an absorbing particle without thermal contact with the substrate, the second term on the left hand side of (19) can be ignored and then the rate of expansion of the particle is given by

$$\dot{r}=\frac{\beta_p r\sigma_a}{3c_p m_p}I\le\frac{\beta_p I_a}{4c_p\varrho_p}. \tag{20}$$

The case when there is thermal contact with the particle is considered below.

Using the material parameters listed in Tables 1, 3, 4, 5 and it is possible to plot the displacement as a function of time for the three substrates. This has been done in Figs. 3, 4 and 5 for a laser pulse having $\tau = 8.1$ ns and fluence equal to that of the threshold fluence for each substrate. The plots show the substrate displacement along with the particle expansion and the total displacement plotted against time for each substrate. They show that, in the case of silica, the total displacement is due entirely to particle expansion. With silicon, the displacement is predominantly due to substrate expansion, although there is a significant contribution from the particles. With glass, the contribution of particle expansion to the total displacement is smaller still.

The equation of motion (15) can be solved numerically to find the fluence required to detach the particle (detachment occurs when $h = 0$). Table 6 gives the calculated threshold fluences for glass and silica substrates for a range of particle

Specific heat, c_s	$720\,\mathrm{J\,kg^{-1}\,K^{-1}}$
Volumetric thermal expansion, β_s	$7.7\times10^{-6}\,\mathrm{K^{-1}}$
Poisson ratio, σ_s	0.27
Young's modulus, E_s	$1.6\times10^{11}\,\mathrm{Nm^{-2}}$
Density, ϱ_s	$2300\,\mathrm{kg\,m^{-3}}$
Absorption coefficient, α_s	$1.67\times10^{8}\,\mathrm{m^{-1}}$
Reflectivity, R_s	0.61

TABLE 5 Material values for silicon from [13]

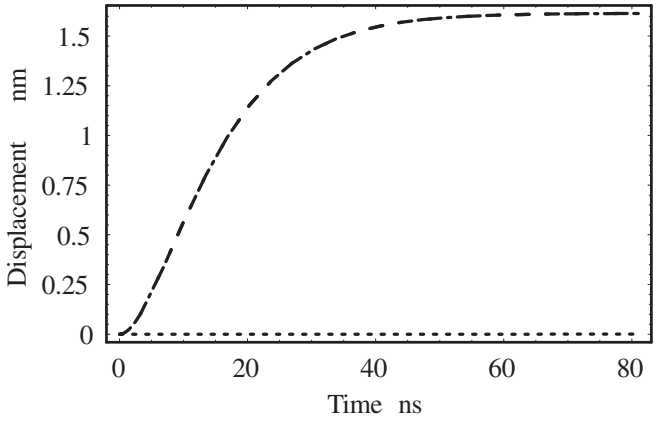

FIGURE 2 A plot showing the normalized displacement of silicon (*dashes*), glass (*solid*) and silica (*dots/dashes*) substrates as a function of time ($\phi = 461\ \mathrm{mJ/cm^2}$, $\tau = 8.1$ ns)

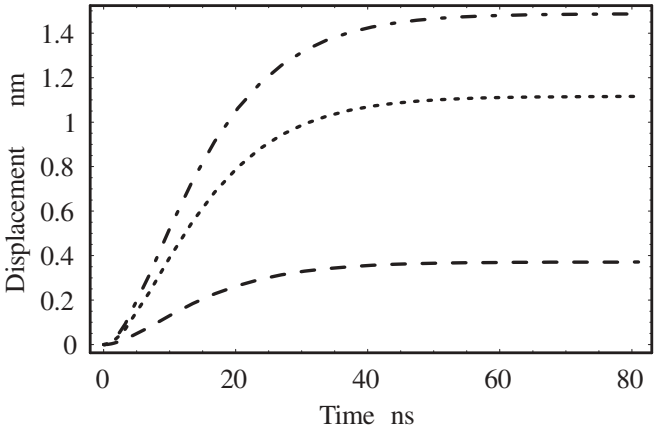

FIGURE 3 A plot showing the calculated displacement of silica substrate (*dots*), expansion of a 3.0 μm sized alumina particle (*dashes*) and the combined displacement (*dots/dashes*–note that this line coincides with the *dashed line*) as a function of time (no thermal contact, $\phi = 461\ \mathrm{mJ/cm^2}$, $\tau = 8.1$ ns)

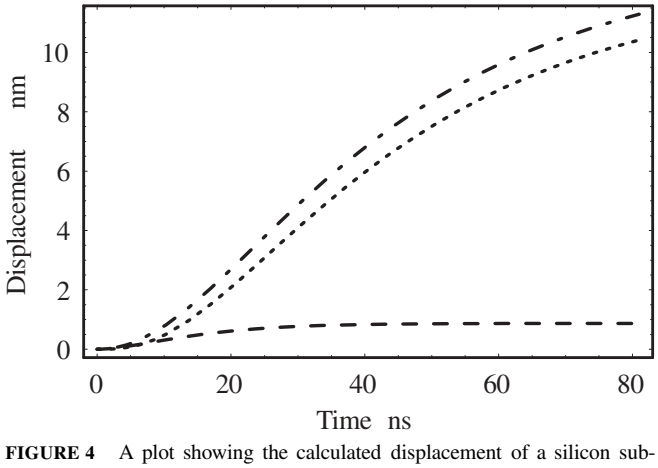

FIGURE 4 A plot showing the calculated displacement of a silicon substrate (*dots*), expansion of a 3.0 μm sized alumina particle (*dashes*) and the combined displacement (*dots/dashes*) as a function of time (no thermal contact, $\phi = 106\ \mathrm{mJ/cm^2}$, $\tau = 8.1$ ns)

absorptivity values. A range of values is used because the particle absorption cannot be determined with precision.

The experimentally measured value of the particle absorptivity is 0.16 and gives threshold fluences of the right order

Particle Absorptivity	Silica Threshold Fluence ($\mathrm{mJ/cm^2}$)	Glass Threshold Fluence ($\mathrm{mJ/cm^2}$)	Ratio of Silica to Glass Threshold Fluences
0.001	74036.6	308.9	239.7
0.0025	29597.9	308.7	95.9
0.005	14804.6	308.2	48.0
0.016	4626.3	306.3	15.1
0.03	2467.3	303.1	8.1
0.16	462.4	251.8	1.8
0.5	148.0	136.1	1.1
1.0	74.0	72.9	1.0

TABLE 6 Dependence of the threshold fluences of glass and silica slides on particle absorptivity for a 3.0 μm particle with no thermal contact between the substrate and particle

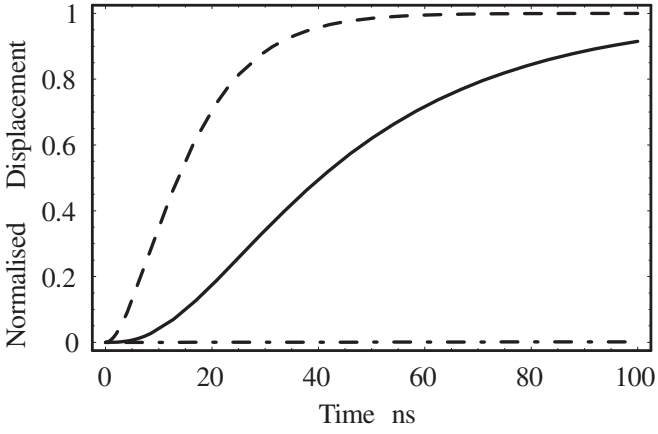

FIGURE 5 A plot showing the calculated displacement of a glass substrate (*dots*), expansion of 3.0 μm sized alumina particles (*dashes*) and the combined displacement (*dots/dashes*) as a function of time (no thermal contact, $\phi = 249\ \mathrm{mJ/cm^2}$, $\tau = 8.1$ ns)

of magnitude as those found experimentally (silica was found to have a threshold fluence of $810\ \mathrm{mJ/cm^2}$ while glass microscope slides have a threshold fluence of $100\ \mathrm{mJ/cm^2}$ [16]). However, the ratio of the threshold fluence of silica to that of glass is calculated to be 1.8 with those material properties, whereas the experimental value is 8.1.

It should be noted that the alumina particles used in the experiments were irregular in shape, whereas the model describes only spherical particles. In addition many of the alumina particles formed agglomerates so that in the experiment there were a range of particle sizes present.

A particle absorptivity of 0.03 gives a ratio of threshold fluences that is close to the experimental one. But when this is the case the absolute values of the fluences are about 3 times greater than those observed experimentally.

In this region of low particle absorptivities the ratio of the threshold fluences of silica to glass is effectively inversely proportional to the particle absorptivity. This is because the glass threshold fluence approaches a limiting value of $309.0\ \mathrm{mJ/cm^2}$ as the particle absorptivity tends to zero. Silica, on the other hand, even at low particle absorptivities has no noticeable contribution from substrate expansion. Thus halving the value of the particle absorptivity results in a doubling of the threshold fluence.

Comparing these numerical results with those obtained using the quasi-static approximation in [16] it is apparent that the latter underestimate the absolute threshold fluence

and overestimate the ratio of the threshold fluences. The reverse is true of the results obtained by considering dynamic expansion. In the case of the quasi-static approximation, the observed silica to glass threshold ratio is obtained with a particle absorptivity of 0.35.

The model in the form presented here appears to underestimate substrate expansion. There may exist some mechanisms that enhance substrate expansion that are not taken into account by the model. Possible candidates for such a role include:

(i) multiple reflections of laser light within the substrate;
(ii) departure from 1D approximation;
(iii) thermal contact between the particle and the substrate;
(iv) 3D focussing of radiation by particles;

Multiple reflections within a substrate will become significant when the thickness of the substrate, d, is comparable with the absorption length, l_α. In this case, the total amount of light absorbed will increase by a factor of $(1 - R_\mathrm{s}\exp(-\alpha_\mathrm{s} d))^{-1}$ compared to the amount absorbed by a slab of a finite thickness neglecting multiple reflections. For glass microscope slides this factor is 1.0021, while for fused silica slides it is 1.042. In both cases, it is close to unity and cannot explain the disparity between the theoretical and experimentally observed threshold fluences.

The model given in this paper is a one dimensional model. Three dimensional elastic effects will become significant when the sound leaves the irradiated area in the lateral direction, i.e. when $w_0 < v_\mathrm{s}\tau$. Departure from one-dimensionality may increase the displacement of the substrate [13]. For the laser used in this experiment $v_\mathrm{s}\tau$ is 47.3 μm, whereas the laser beam dimensions are 7 mm by 3 mm. Thus, a 1D model should be a good approximation in this case.

In the model presented above, it was assumed that there was no thermal contact between the particle and the substrate. With absorbing particles and transparent substrates the particles will transfer heat to the substrate resulting in enhancement of substrate expansion at the expense of particle expansion. As mentioned above, this is just what is required to explain the observed experimental results.

Substituting (9) with $z = 0$ into (19) and solving for T_p gives

$$T_\mathrm{p}(t) = \mathrm{e}^{-\gamma_\mathrm{p} t}\left\{\frac{\sigma_\mathrm{a}}{c_\mathrm{p} m_\mathrm{p}}\frac{I_0}{\tau}\left(\frac{t\mathrm{e}^{(\gamma_\mathrm{p}-1/\tau)t}}{\gamma_\mathrm{p}-1/\tau} - \frac{\mathrm{e}^{(\gamma_\mathrm{p}-1/\tau)t}-1}{(\gamma_\mathrm{p}-1/\tau)^2}\right)\right.$$
$$+\frac{\gamma_\mathrm{p} I_0 \alpha_\mathrm{s}\tau}{\varrho_\mathrm{s} c_\mathrm{s}}\left(\frac{\mathrm{e}^{\gamma_\mathrm{p} t}-1}{\gamma_\mathrm{p}} - \frac{\mathrm{e}^{(\gamma_\mathrm{p}-1/\tau)t}-1}{\gamma_\mathrm{p}-1/\tau} - \frac{t}{\tau}\frac{\mathrm{e}^{(\gamma_\mathrm{p}-1/\tau)t}}{\gamma_\mathrm{p}-1/\tau}\right.$$
$$\left.\left.+\frac{1}{\tau(\gamma_\mathrm{p}-1/\tau)^2(\mathrm{e}^{(\gamma_\mathrm{p}-1/\tau)t}-1)}\right)\right\} \qquad (21)$$

where $\gamma_\mathrm{p} = 4K_\mathrm{s} a/(c_\mathrm{p} m_\mathrm{p})$.

The transfer of heat from the particle to the substrate will result in local 3D heating of the substrate. This can be approximated by modelling it as an effective Gaussian beam with spot size a and $P = \pi a^2 I_\mathrm{3D} = 4K_\mathrm{s} a\,(T_\mathrm{p} - T_\mathrm{s})$ so that

$$I_\mathrm{3D} = \frac{4}{\pi}\frac{K_\mathrm{s}(T_\mathrm{p} - T_\mathrm{s})}{a}\,. \qquad (22)$$

This will give rise to a temperature rise in the substrate given by

$$T_\mathrm{s3D}(0,t) = \frac{1}{\sqrt{\pi} c_\mathrm{s}\varrho_\mathrm{s}}\int_0^t \frac{I_\mathrm{3D}(t-t_1)}{\sqrt{D_\mathrm{s} t_1}(1+4D_\mathrm{s} t_1/a^2)}\mathrm{d}t_1\,. \qquad (23)$$

The resulting local 3D expansion of the substrate will be [22]

$$\dot{l}_\mathrm{3D} \approx \frac{2\beta_\mathrm{s}(1+\sigma)}{3c_\mathrm{s}\varrho_\mathrm{s}}\left[\int_0^t \frac{\dot{I}_\mathrm{3D}(t-t_1)}{1+8D_\mathrm{s} t_1/a^2}\,\mathrm{d}t_1\right] \qquad (24)$$

The temperatures of the substrate and particle have been plotted for glass in Figs. 6 and 7 both with and without thermal contact. In the case of thermal contact, the contribution to the substrate temperature rise by heating from the particle is also shown. This figure shows that there is little difference to the temperature of the particle, but there is significant localized heating of the substrate by the particle. The plots for silica and silicon are similar. Figure 8 shows the displacement against time plot for glass when thermal contact is accounted

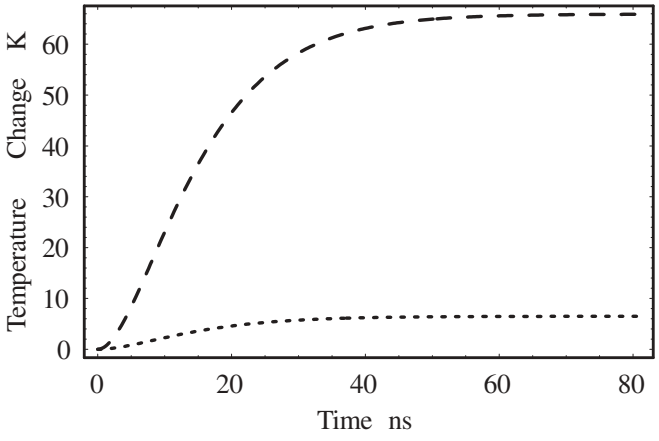

FIGURE 6 A plot showing the calculated temperature of a glass substrate (*dots*) and a 3.0 μm sized alumina particle (*dashes*) as a function of time ignoring thermal contact between particle and substrate ($\phi = 249\,\mathrm{mJ/cm^2}$, $\tau = 8.1$ ns)

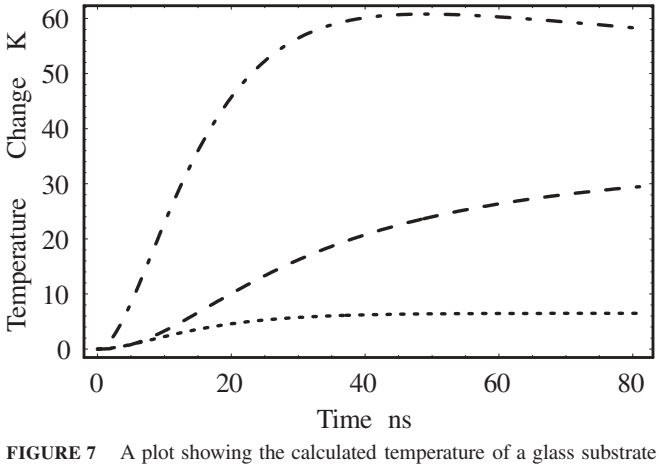

FIGURE 7 A plot showing the calculated temperature of a glass substrate (*dots*), a 3.0 μm sized alumina particle (*dots/dashes*) and the temperature rise at the substrate due to thermal contact with the particle (*dashes*) ($\phi = 249\,\mathrm{mJ/cm^2}$, $\tau = 8.1$ ns)

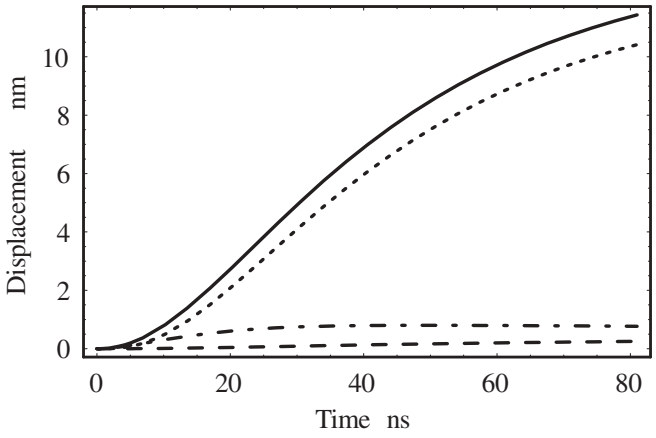

FIGURE 8 A plot showing the calculated displacement of a glass substrate (1D component–*dots*, 3D component–*dashes*) and a 3.0 μm sized alumina particle (*dots*/*dashes*) together with the total displacement (*solid line*) as a function of time taking into account thermal contact between particle and substrate ($\phi = 249$ mJ/cm^2, $\tau = 8.1$ ns)

for. There is very little difference from the equivalent plot for when thermal contact is ignored (see Fig. 4). The plots for silica shows very little variation from the plots without thermal contact but the plot for silicon does show significant differences in this case.

To calculate the effect that thermal contact between the particle and the substrate has on threshold fluence, l_{3D} needs to be incorporated into the equation of motion (15) together with the modified expression for r that can be obtained by combining (21) and (18). Table 7 shows the dependence of the threshold fluence on particle absorptivity for this case. Comparing this Table with Table 6, it can be seen that thermal contact decreases the threshold fluences by a small amount. This is due to the particle heating the substrate, thus increasing its expansion. For example, there is a 1.3% reduction in threshold fluence for a 1.5 μm particle having an absorptivity of 0.16 on a glass microscope slide when thermal contact is taken into consideration. This variation in threshold fluence is insensitive to contact area. If a contact radius of 1.5 μm is used (i.e. the particle is perfectly flat) the reduction in threshold fluence when thermal contact is accounted for is 1.2%.

So it would appear that thermal contact alone cannot account for the discrepancy between the calculated threshold fluences and the experimentally observed ones and that there must be some other mechanism which enhances substrate expansion.

The last candidate for such a mechanism is the 3D focussing of radiation by particles. This effect was modelled theoretically and was shown to strongly influence laser cleaning efficiency in the case of transparent, spherical particles. It can cause local field enhancement of over 30 times [23]. It is not obvious how this effect could be extended to apply to irregular, absorbing particles. The intensity enhancement near arbitrary shaped particles certainly exists and may reach a factor of two or more [24]. This would have the effect of lowering the threshold fluence by about the same amount. In this way, the particle absorptivity of 0.03 will have the same ratio of threshold fluence for silica and glass and give more realistic absolute values of threshold fluences. But further work needs to be done to incorporate this effect into the model.

On the experimental side, it would be useful to try using other particles and other substrates having a range of absorptivities. In particular, comparison of two different glasses with significantly different absorption at 248 nm will be tested in the future.

Particle Absorptivity	Silica Threshold Fluence (mJ/cm^2)	Glass Threshold Fluence (mJ/cm^2)	Ratio of Silica to Glass Threshold Fluences
0.001	73806.9	308.7	239.1
0.0025	29524.4	308.6	95.7
0.005	14757.9	308.1	47.9
0.016	4613.2	305.9	15.1
0.03	2459.6	302.6	8.1
0.16	461.2	248.5	1.9
0.5	147.6	131.7	1.1
1.0	73.8	70.4	1.1

TABLE 7 Calculated dependence of the threshold fluences of glass and silica slides on particle absorptivity for a 3.0 μm particle with thermal contact between the substrate and particle

5 Conclusions

It has been shown that for substrates with relatively low absorptivities, like silica and glass, dynamic considerations can potentially substantially reduce thermal expansion of the substrate caused by irradiation by nanosecond laser pulses compared with quasi-static expansion. In particular, the expansion of the substrate occurs over a much longer time frame than that assumed by the quasi-static approximation. Consequently, acceleration of the substrate surface is greatly reduced and laser cleaning thresholds are increased.

The predictions of the model of Arnold et al. when adjusted for dynamic considerations that take into account the finite velocity of sound, give reasonable agreement with experimentally found threshold fluences for alumina particles on silica and glass substrates, although it underestimates the ratio of the threshold fluences between silica and glass. This could be due to the model's underestimating of the contribution of surface expansion to the laser cleaning process or due to the irregularly shaped particles used in the experiments. The influence of multiple reflections in the substrate and departure from one dimensionality was found to be insignificant. Thermal contact between the particle and the substrate was also found to have little effect on laser cleaning threshold fluences. The most likely substrate enhancement mechanism appears to be the near-field effect.

ACKNOWLEDGEMENTS This research was supported by an Australian Research Council Large Grant and Fonds zur Förderung der wissenschaftlichen Forschung in Österreich, project P14700-TPH. We also thank Prof. D. Bäuerle for many fruitful discussions.

REFERENCES

1 D.M. Kane, A.J. Fernandes, D.R. Halfpenny: In: *Laser Cleaning*, ed. by B. Luk'yanchuk (World Scientific, New Jersey, London 2002), Chapt. 4, pp. 181–228
2 D.R. Halfpenny, D.M. Kane: J. Appl. Phys. **86**, 6641 (1999)
3 D.M. Kane, A.J. Fernandes: Proc. SPIE **4426**, 334 (2001)
4 A.J. Fernandes, D.M. Kane: Proc. SPIE **4426**, 290 (2001)
5 V. Dobler et al.: Appl. Phys. A **69**, 335 (1999)

6 Y.F. Lu et al.: Appl. Phys. A **65**, 9 (1997)
7 Y.F. Lu, Y.W. Zheng, W.D. Song: Appl. Phys. A **68**, 569 (1999)
8 Y.F. Lu et al.: J. Appl. Phys. **80**, 499 (1996)
9 A.A. Kolomenskii, H.A. Schuessler, V.G. Mikhalevich, A.A. Maznev: J. Appl. Phys. **84**, 2404 (1998)
10 Y.F. Lu, Y.W. Zheng, W.D. Song: J. Appl. Phys. **87**, 549 (2000)
11 G. Vereecke, E. Rohr, M.M. Heyns: J. Appl. Phys. **85**, 3837 (1999)
12 B.S. Luk'yanchuk, Y.W. Zheng, Y.F. Lu: RIKEN Review **43**, 28 (2002)
13 N. Arnold et al.: Proc. SPIE **4426**, 340 (2002)
14 N. Arnold: In: *Laser Cleaning*, ed. by B.S. Luk'yanchuk (World Scientific, New Jersey, London 2002) Chapt. 2, pp. 51–102
15 N. Arnold: Appl. Surf. Sci. **197–198**, 904 (2002)
16 S. Pleasants, D.M. Kane: J. Appl. Phys. **93**, 8862 (2002)
17 D. Bauerle: *Laser Processing and Chemistry*, 3rd edn. (Springer-Verlag, Berlin 2000)
18 A.A. Maznev, J. Hohlfeld, J. Gudde: J. Appl. Phys. **82**, 5082 (1997)
19 D.R. Halfpenny, Ph.D. thesis: Macquarie University (1999)
20 M.E. Innocenzi et al.: J. Appl. Phys. **67**, 7542 (1990)
21 C.F. Bohren, D.R. Huffman: *Absorption and Scattering of Light from Small Particles* (Wiley, New York 1998)
22 N. Arnold: Appl. Surf. Sci. **208–209**, 15 (2003)
23 B.S. Luk'yanchuk, Y.W. Zheng, Y.F. Lu: Proc. SPIE **4065**, 576 (2000)
24 B.S. Luk'yanchuk et al.: In: *Laser Cleaning*, ed. by B.S. Luk'yanchuk (World Scientific, New Jersey, London 2002) Chapt. 3, pp. 103–178
25 D.N. Nikogosyan: *Properties of Optical and Laser-Related Materials – a Handbook* (Wiley, New York 1997)